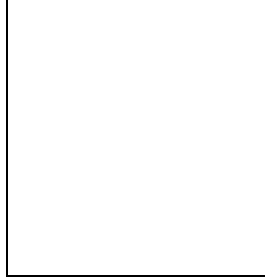


# Lepton Flavor Violating $\tau$ and $\mu$ decays

E. Arganda, M.J. Herrero

*Departamento de Física Teórica, UAM/IFT, 28049, Madrid, Spain*



In this work the following lepton flavor violating  $\tau$  and  $\mu$  decays are studied:  $\tau^- \rightarrow \mu^- \mu^- \mu^+$ ,  $\tau^- \rightarrow e^- e^- e^+$ ,  $\mu^- \rightarrow e^- e^- e^+$ ,  $\tau^- \rightarrow \mu^- \gamma$ ,  $\tau^- \rightarrow e^- \gamma$  and  $\mu^- \rightarrow e^- \gamma$ . We work in a constrained supersymmetric scenario with universal soft breaking terms and where the MSSM particle content is extended by the addition of three heavy right handed Majorana neutrinos and their supersymmetric partners. The generation of neutrino masses is done via the seesaw mechanism. We analyze all these lepton flavor violating decays in terms of the relevant input parameters, which are the usual mSUGRA parameters and the seesaw parameters. In the numerical analysis compatibility with the most recent experimental upper bounds on all these  $\tau$  and  $\mu$  decays, with the neutrino data, and with the present lower bounds on the supersymmetric particle masses are required. Two typical scenarios with degenerate and hierarchical heavy neutrinos are considered. We will show here that the minimal supergravity and seesaw parameters do get important restrictions from these  $\tau$  and  $\mu$  decays in the hierarchical neutrino case.

## 1 Introduction

The present strong evidence for lepton flavor changing neutrino oscillations in neutrino data implies the existence of non-zero masses for the light neutrinos, and provides the first experimental clue for physics beyond the Standard Model (SM). This fact does require a theoretical framework beyond the SM with just three massless left-handed neutrinos. Within the MSSM-seesaw context, which will be adopted here, the MSSM particle content is enlarged by three right handed neutrinos plus their corresponding supersymmetric (SUSY) partners, and the neutrino masses are generated by the seesaw mechanism. Three of the six resulting Majorana neutrinos have light masses,  $m_{\nu_i}, i = 1, 2, 3$ , and the other three have heavy masses,  $m_{N_i}, i = 1, 2, 3$ . These physical masses can be related to the Dirac mass matrix  $m_D$ , the right-handed neutrino mass matrix  $m_M$ , and the unitary matrix  $U_{MNS}$  by  $\text{diag}(m_{\nu_1}, m_{\nu_2}, m_{\nu_3}) \simeq U_{MNS}^T (-m_D m_M^{-1} m_D^T) U_{MNS}$  and  $\text{diag}(m_{N_1}, m_{N_2}, m_{N_3}) \simeq m_M$ , respectively. Here we have chosen an electroweak eigenstate basis where  $m_M$  and the charged lepton mass matrix are flavor diagonal, and we have assumed that all elements in  $m_D = Y_\nu < H_2 >$ , where  $Y_\nu$  is the neutrino Yukawa coupling matrix and  $< H_2 > = v \sin \beta$  ( $v = 174$  GeV), are much smaller than those of  $m_M$ . The two previous relations can be rewritten together in a more convenient form for the work presented here as,  $m_D^T = i m_N^{\text{diag } 1/2} R m_\nu^{\text{diag } 1/2} U_{MNS}^+$ , where  $R$  is a general complex and orthogonal  $3 \times 3$  matrix, which will be parameterized by three complex angles  $\theta_i, i = 1, 2, 3$ .

One of the most interesting features of the SUSY-seesaw models is the associated rich phenomenology due to the occurrence of lepton flavor violating (LFV) processes. In these models the LFV ratios can be large due to an important source of lepton flavor mixing in the soft-SUSY-breaking terms. Even in the scenarios with universal soft-SUSY-breaking parameters at

the large energy scale associated to the SUSY breaking  $M_X$ , the running from this scale down to  $m_M$  induces, via the neutrino Yukawa couplings, large lepton flavor mixing in the slepton soft masses, and provides the so-called slepton-lepton misalignment, which in turn generates non-diagonal lepton flavor interactions. These interactions can induce sizable ratios in several LFV processes which are actually being tested experimentally with high precision and therefore provide a very interesting window to look for indirect SUSY signals. Among these processes, the LFV  $\tau$  and  $\mu$  decays are probably the most interesting ones for various reasons. On one hand, they get vanishing rates in the SM with massless neutrinos and highly suppressed rates in the SM with massive neutrinos. The smallness of these rates in the non-SUSY version of the seesaw mechanism for neutrino mass generation is due to their suppression by inverse powers of the heavy scale  $m_M$ . On the other hand, although these decays have not been seen so far in the present experiments, there are very restrictive upper bounds<sup>1</sup> on their possible rates which imply important restrictions on the new physics beyond the SM. These restrictions apply severely to the case of softly broken SUSY theories with massive neutrinos and the seesaw mechanism, since these give rise to higher rates, being suppressed by inverse powers of the SUSY breaking scale,  $m_{SUSY} \leq 1$  TeV, instead of inverse powers of  $m_M$ .

Here we compute the partial widths for the LFV  $\tau$  and  $\mu$  decays of type  $l_j \rightarrow l_i \gamma$  and  $l_j \rightarrow 3l_i$  to one-loop order and analyze numerically the corresponding branching ratios in terms of the mSUGRA and seesaw parameters, namely,  $M_0$ ,  $M_{1/2}$ ,  $\tan \beta$ ,  $m_{N_i}$  and  $R$ . To solve numerically the RGEs we use the Fortran code SPheno<sup>2</sup> that we have adapted to include the full flavor structure of the  $3 \times 3$  soft SUSY breaking mass and trilinear coupling matrices and of the Yukawa coupling matrices. Our final goal is to use the SUSY contributions to LFV  $\tau$  and  $\mu$  decays as an efficient way to test the mSUGRA and seesaw parameters and we explore in detail the restrictions imposed from the present experimental bounds. We will find that for some plausible choices of the seesaw parameters, being compatible with neutrino data, there are indeed large excluded regions in the mSUGRA parameter space.

For the numerical analysis, the  $U_{MNS}$  matrix elements and the  $m_{\nu_i}$  are fixed to the most favored values by neutrino data with  $\sqrt{\Delta m_{sol}^2} = 0.008$  eV,  $\sqrt{\Delta m_{atm}^2} = 0.05$  eV,  $\theta_{12} = \theta_{sol} = 30^\circ$ ,  $\theta_{23} = \theta_{atm} = 45^\circ$ ,  $\theta_{13} = 0^\circ$  and  $\delta = \alpha = \beta = 0$ . Some results will also be presented for the alternative choice of small but non-vanishing  $\theta_{13}$ . We consider two plausible scenarios, one with quasi-degenerate light and degenerate heavy neutrinos and with  $m_{\nu_1} = 0.2$  eV,  $m_{\nu_2} = m_{\nu_1} + \frac{\Delta m_{sol}^2}{2m_{\nu_1}}$ ,  $m_{\nu_3} = m_{\nu_1} + \frac{\Delta m_{atm}^2}{2m_{\nu_1}}$  and  $m_{N_1} = m_{N_2} = m_{N_3} = m_N$ ; and the other one with hierarchical light and hierarchical heavy neutrinos, and with  $m_{\nu_1} \simeq 0$  eV,  $m_{\nu_2} = \sqrt{\Delta m_{sol}^2}$ ,  $m_{\nu_3} = \sqrt{\Delta m_{atm}^2}$  and  $m_{N_1} \leq m_{N_2} < m_{N_3}$ .

This is a reduced version of our more complete work<sup>3</sup> to which we address the reader for more details.

## 2 Numerical results and conclusions

For the degenerate heavy neutrinos case, we have gotten rates for all the studied LFV  $\tau$  and  $\mu$  decays that are below the present experimental upper bounds, and we are basically in agreement with previous results<sup>4</sup>. The largest rates we get, within the explored range of the seesaw and mSUGRA parameter space, are for the  $\tau$  decays. Specifically,  $\text{BR}(\tau \rightarrow \mu \gamma) \sim 10^{-8}$  and  $\text{BR}(\tau^- \rightarrow \mu^- \mu^- \mu^+) \sim 3 \times 10^{-11}$ , corresponding to the extreme values of  $\tan \beta = 50$  and  $m_N = 10^{14}$  GeV and for the lowest values of  $M_0$  and  $M_{1/2}$  explored. The case of hierarchical heavy neutrinos turns out to be much more interesting. First of all, we get much larger branching ratios than in the previous case and secondly they are in many cases above the present experimental bounds.

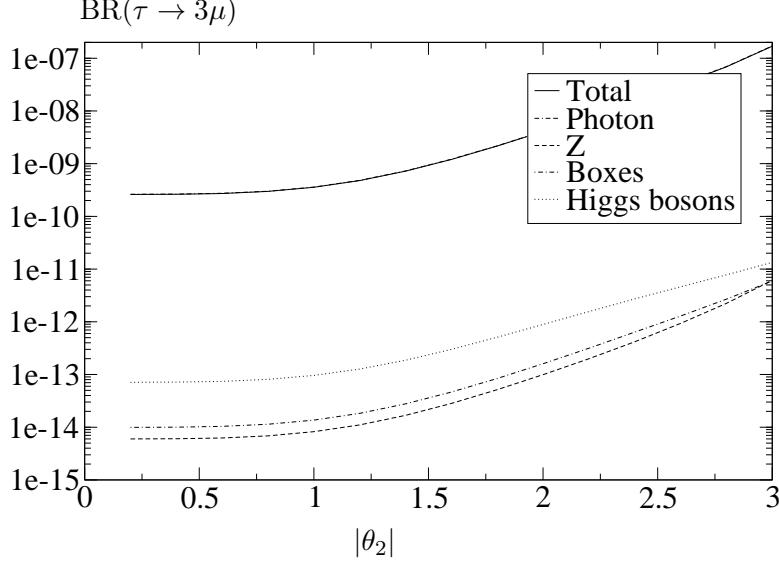


Figure 1: Dependence of  $\text{BR}(\tau^- \rightarrow \mu^- \mu^- \mu^+)$  with  $|\theta_2|$  for  $\arg(\theta_2) = \pi/4$ ,  $(m_{N_1}, m_{N_2}, m_{N_3}) = (10^8, 2 \times 10^8, 10^{14})$  GeV,  $\theta_1 = \theta_3 = 0$ ,  $\tan \beta = 50$ ,  $M_0 = 400$  GeV,  $M_{1/2} = 300$  GeV,  $A_0 = 0$  and  $\text{sign}(\mu) > 0$ .

For the more interesting hierarchical case we show in Figs. 1-5 the numerical results for the branching ratios of the LFV  $\tau$  and  $\mu$  decays for both types,  $l_j \rightarrow 3l_i$  and the correlated radiative decays  $l_j \rightarrow l_i \gamma$ . All the LFV  $\tau$  and  $\mu$  decay rates are mainly sensitive to  $\tan \beta$ , the heaviest neutrino mass  $m_{N_3}$ , which we have set in these figures to  $m_{N_3} = 10^{14}$  GeV, and the complex angles in the  $R$  matrix  $\theta_1$  and  $\theta_2$ , which have been taken in the range  $3 < \tan \beta < 50$ ,  $0 < |\theta_i| < 3$  and  $0 < \arg(\theta_i) < \pi/4$ . In Fig. 1 we show separately the various contributions to  $\text{BR}(\tau^- \rightarrow \mu^- \mu^- \mu^+)$  as a function of  $|\theta_2|$ . The dominant one is the photon-penguin contribution (which is undistinguishable from the total in this figure) and the others (Z-penguin, H-penguin and boxes) are several orders of magnitude smaller. All the rates for  $\tau^- \rightarrow \mu^- \mu^- \mu^+$  in this plot are within the allowed range by the experimental bound, which is placed just at the upper line of the rectangle. In contrast, we have obtained that, for the mSUGRA and seesaw parameters of Fig. 1, the predicted  $\text{BR}(\tau \rightarrow \mu \gamma)$  is above the experimental bound for the explored range of  $0 < |\theta_2| < 3$ . In Fig. 2 we show the predictions of  $\text{BR}(l_j^- \rightarrow l_i^- l_i^- l_i^+)$  and  $\text{BR}(l_j \rightarrow l_i \gamma)$  as functions of  $|\theta_2|$ , for all the channels and for different values of  $\arg(\theta_2)$ . It is clear that all the branching ratios have a soft behaviour with  $|\theta_2|$  except for the case of real  $\theta_2$  where appears a narrow dip in each plot. In this Fig. 2 we see that all the rates obtained are below their experimental upper bounds, except for the processes  $\tau \rightarrow \mu \gamma$  and  $\mu \rightarrow e \gamma$ , where the predicted rates for complex  $\theta_2$  with large  $|\theta_2|$  are clearly above the allowed region. The most restrictive channel in this case is  $\tau \rightarrow \mu \gamma$  where compatibility with data occurs just for real  $\theta_2$  and for complex  $\theta_2$  but with  $|\theta_2|$  values near the region of the narrow dip. We also see that the rates for  $\text{BR}(\mu \rightarrow 3e)$  enter in conflict with experiment at the upper corner of large  $|\theta_2|$  and large  $\arg(\theta_2) = \pi/4$ . Even more interesting are the predictions for  $\text{BR}(l_j^- \rightarrow l_i^- l_i^- l_i^+)$  and  $\text{BR}(l_j \rightarrow l_i \gamma)$  as functions of  $|\theta_1|$ , due to the large values of the relevant entries of the  $Y_\nu$  coupling matrix. Concretely,  $|Y_\nu^{13}|$  can be as large as  $\sim 0.2$  for  $|\theta_1| \sim 2.5$  and  $\arg(\theta_1) = \pi/4$ , and  $|Y_\nu^{23}|$  and  $|Y_\nu^{33}|$  are in the range  $0.1 - 1$  for all studied complex  $\theta_1$  values. The results for  $\text{BR}(l_j^- \rightarrow l_i^- l_i^- l_i^+)$  and  $\text{BR}(l_j \rightarrow l_i \gamma)$  as functions of  $|\theta_1|$ , for different values of  $\arg(\theta_1)$ , are illustrated in Fig. 3. We see clearly that the restrictions are more severe in this case than in the previous one. In fact, all the rates cross the horizontal lines of the experimental bounds except for  $\text{BR}(\tau^- \rightarrow \mu^- \mu^- \mu^+)$  and  $\text{BR}(\tau^- \rightarrow e^- e^- e^+)$ . The most restrictive channel is now the  $\mu \rightarrow e \gamma$  decay. More specifically, we see that all the points in the plot of  $\text{BR}(\mu \rightarrow e \gamma)$ , except for the particular values  $\theta_1 = 0$  and real  $\theta_1$  at the dip, are

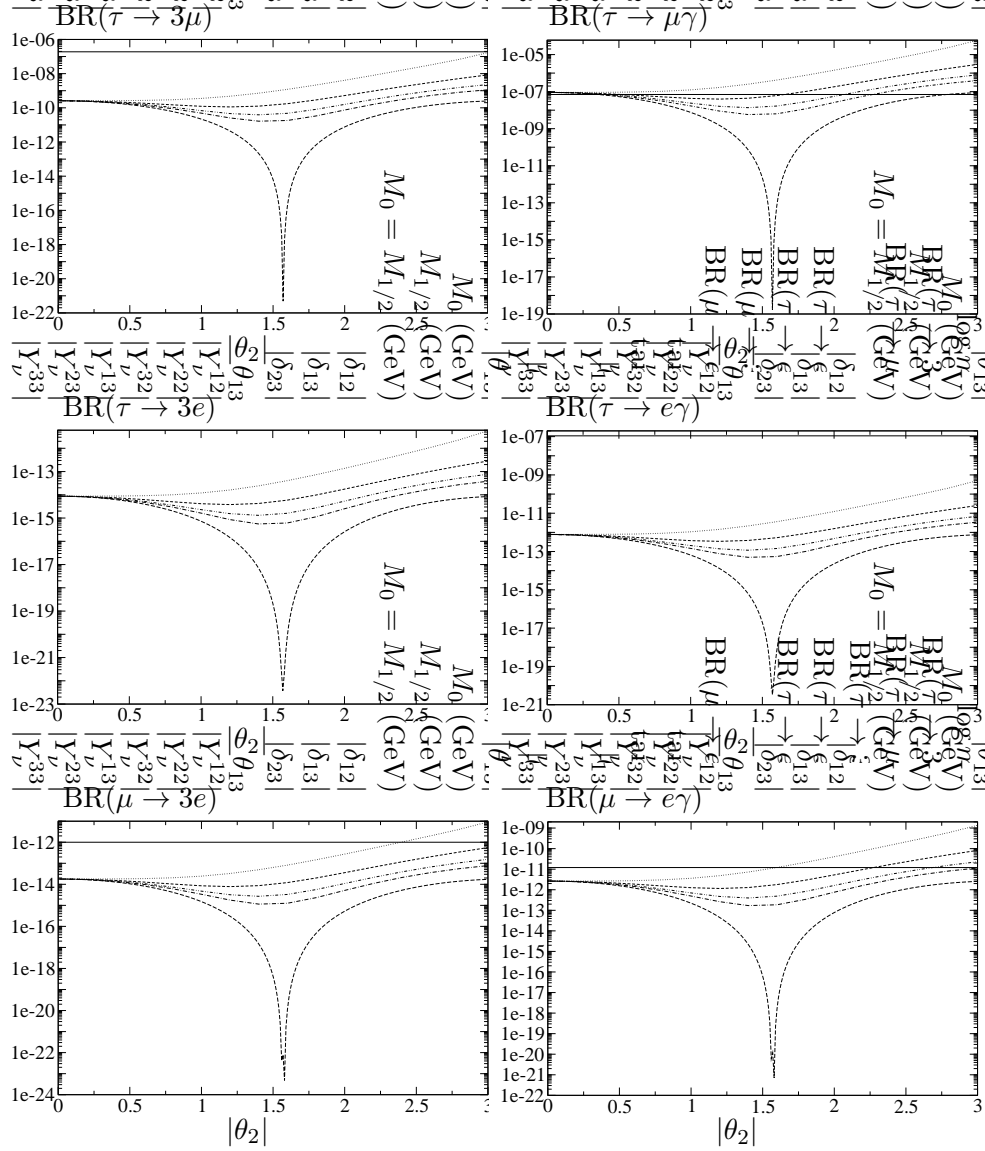


Figure 2: Dependence of LFV  $\tau$  and  $\mu$  decays with  $|\theta_2|$  with hierarchical heavy neutrinos and complex R, for  $\arg(\theta_2) = 0, \pi/10, \pi/8, \pi/6, \pi/4$  in radians (lower to upper lines),  $(m_{N_1}, m_{N_2}, m_{N_3}) = (10^8, 2 \times 10^8, 10^{14})$  GeV,  $\theta_1 = \theta_3 = 0$ ,  $\tan \beta = 50$ ,  $M_0 = 400$  GeV,  $M_{1/2} = 300$  GeV,  $A_0 = 0$  and  $\text{sign}(\mu) > 0$ . The horizontal lines are the upper experimental bounds.

excluded by the experimental upper bound. Also the predictions for  $BR(\mu \rightarrow 3e)$  are mostly excluded, except again for the region close to zero and the dip. We have also explored the dependence with the complex  $\theta_3$  angle, and it turns out that the predictions for all rates are nearly constant with this angle. We have also tried another input values for the heavy neutrino masses. The results for  $BR(\tau \rightarrow 3\mu)$  are shown in Fig. 4. Here we compare the predictions for the three following set of values,  $(m_{N_1}, m_{N_2}, m_{N_3}) = (10^8, 2 \times 10^8, 10^{14})$  GeV,  $(10^{10}, 2 \times 10^{10}, 10^{14})$  GeV and  $(10^8, 2 \times 10^8, 10^{12})$  GeV. We conclude, that the relevant mass is the heaviest one,  $m_{N_3}$ , and the scaling with this mass is approximately as the scaling with the common mass  $m_N$  in the degenerate case, namely,  $(m_{N_3} \log m_{N_3})^2$ . Because of this, the rates for the two first sets are nearly undistinguishable, and the rates for the third set are about four orders of magnitude below. Finally, we consider the very interesting case where the angle  $\theta_{13}$  of the  $U_{MNS}$  is non vanishing. It is known that the present neutrino data still allows for small values of this angle,  $\theta_{13} < 10^\circ$ . The dependence of  $BR(\mu^- \rightarrow e^- e^- e^+)$  and  $BR(\mu \rightarrow e\gamma)$  with this  $\theta_{13}$  is shown in Fig. 5 where we explore values in the  $0 < \theta_{13} < 10^\circ$  range. We choose these two channels because they are very sensitive to this angle and because they have the most restrictive experimental bounds. For this study we assume the simplest choice of  $R = 1$ , and set the other parameters to the following

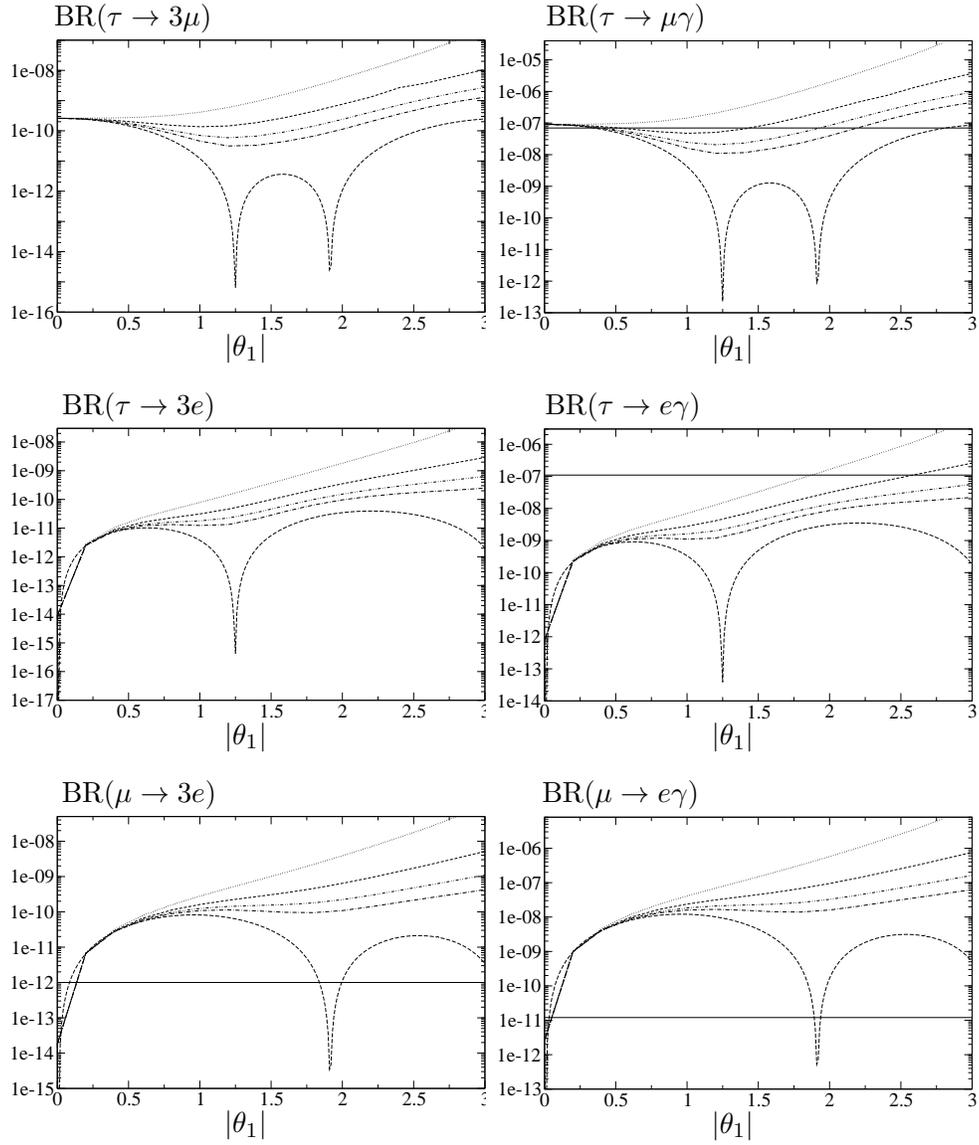


Figure 3: Dependence of LFV  $\tau$  and  $\mu$  decays with  $|\theta_1|$  with hierarchical heavy neutrinos and complex R, for  $\arg(\theta_1) = 0, \pi/10, \pi/8, \pi/6, \pi/4$  in radians (lower to upper lines),  $(m_{N_1}, m_{N_2}, m_{N_3}) = (10^8, 2 \times 10^8, 10^{14})$  GeV,  $\theta_2 = \theta_3 = 0$ ,  $\tan \beta = 50$ ,  $M_0 = 400$  GeV,  $M_{1/2} = 300$  GeV,  $A_0 = 0$  and  $\text{sign}(\mu) > 0$ . The horizontal lines are the upper experimental bounds.

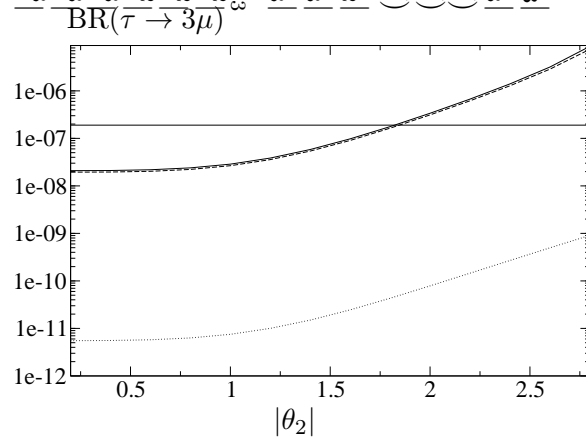


Figure 4: Dependence of LFV  $\tau \rightarrow 3\mu$  with  $|\theta_2|$  in with hierarchical heavy neutrinos, for different  $m_{N_i}$  choices. Solid line is for  $(m_{N_1}, m_{N_2}, m_{N_3}) = (10^8, 2 \times 10^8, 10^{14})$  GeV, dashed line is for  $(m_{N_1}, m_{N_2}, m_{N_3}) = (10^{10}, 2 \times 10^{10}, 10^{14})$  GeV, and dotted line is for  $(m_{N_1}, m_{N_2}, m_{N_3}) = (10^8, 2 \times 10^8, 10^{12})$  GeV. The rest of parameters are set to  $\tan \beta = 50$ ,  $M_0 = 200$  GeV,  $M_{1/2} = 100$  GeV,  $A_0 = 0$ ,  $\text{sign}(\mu) > 0$  and  $\arg(\theta_2) = \pi/4$ . The horizontal line is the experimental bound.

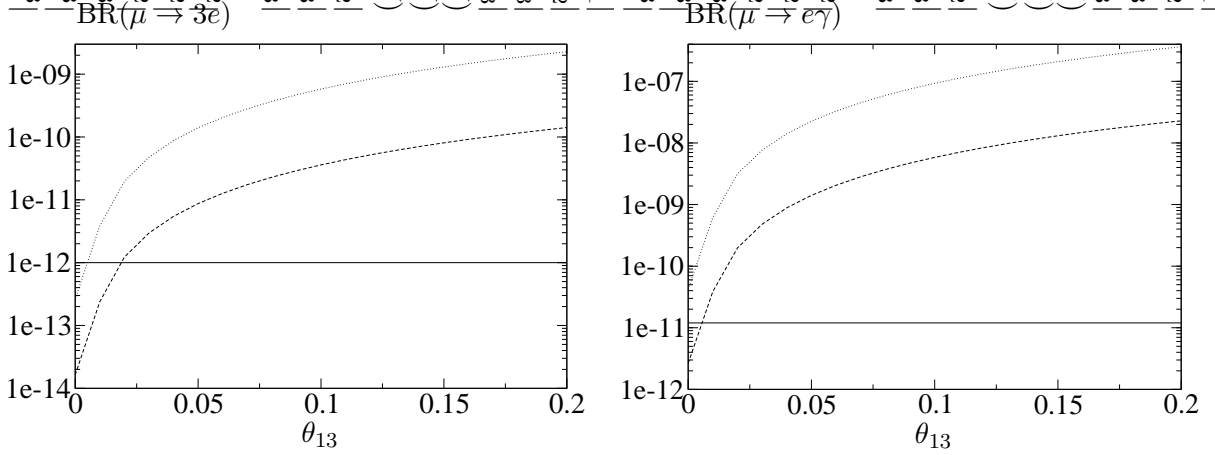


Figure 5: Dependence of LFV  $\mu$  decays with  $\theta_{13}$  in radians with hierarchical heavy neutrinos and  $R = 1$ , for  $(m_{N_1}, m_{N_2}, m_{N_3}) = (10^8, 2 \times 10^8, 10^{14})$  GeV,  $\tan\beta = 50$ ,  $A_0 = 0$  and  $\text{sign}(\mu) > 0$ . The upper lines are for  $M_0 = 250$  GeV,  $M_{1/2} = 150$  GeV and the lower lines are for  $M_0 = 400$  GeV,  $M_{1/2} = 300$  GeV. The horizontal lines are the experimental bounds.

values:  $\tan\beta = 50$ ,  $A_0 = 0$ ,  $\text{sign}(\mu) > 0$ , and  $(m_{N_1}, m_{N_2}, m_{N_3}) = (10^8, 2 \times 10^8, 10^{14})$  GeV. The upper lines are for  $M_0 = 250$  GeV,  $M_{1/2} = 150$  GeV and the lower ones for  $M_0 = 400$  GeV,  $M_{1/2} = 300$  GeV. We conclude that, for this choice of parameters, values of  $\theta_{13}$  in the upper region of the interval  $0 < \theta_{13} < 10^\circ$  are clearly disfavored by the data on LFV  $\mu$  decays. It is a quite striking result.

In summary, we obtain in the hierachical case much larger rates than in the degenerate one, and one must pay attention to these values, because the rates in several channels do get in conflict with the experimental bounds. More specifically, the choice of a complex  $R$  matrix with large modules and/or large arguments of  $\theta_1$  and/or  $\theta_2$  and a light SUSY spectrum is very constrained by data. We also confirm that the experimental upper bounds of the processes  $l_j \rightarrow l_i \gamma$  are more restrictive than the  $l_j^- \rightarrow l_i^- l_i^- l_i^+$  ones but all together will allow to extract large excluded regions of the mSUGRA and seesaw parameter space. A more precise conclusion on the excluded regions of this parameter space deserves a more devoted study.

## Acknowledgments

E. Arganda wishes to thank J.M. Frere for the invitation to the conference and all the organizers for a very fruitful, interesting and enjoyable meeting.

## References

1. B. Aubert *et al.* [BABAR Collaboration], Phys. Rev. Lett. **92**, 121801 (2004) [arXiv:hep-ex/0312027]; U. Bellgardt *et al.* [SINDRUM Collaboration], Nucl. Phys. B **299**, 1 (1988); B. Aubert *et al.* [BABAR Collaboration], Phys. Rev. Lett. **95**, 041802 (2005) [arXiv:hep-ex/0502032]; B. Aubert *et al.* [BABAR Collaboration], arXiv:hep-ex/0508012; M. L. Brooks *et al.* [MEGA Collaboration], Phys. Rev. Lett. **83** (1999) 1521 [arXiv:hep-ex/9905013].
2. W. Porod, Comput. Phys. Commun. **153**, 275 (2003) [arXiv:hep-ph/0301101].
3. E. Arganda and M. J. Herrero, Phys. Rev. D **73**, 055003 (2006) [arXiv:hep-ph/0510405].
4. J. Hisano, T. Moroi, K. Tobe and M. Yamaguchi, Phys. Rev. D **53** (1996) 2442 [arXiv:hep-ph/9510309].